The Royal Society

Spatial asynchrony and periodic travelling waves in cyclic populations of field voles

Xavier Lambin[1]*, David A. Elston[2], Steve J. Petty[3] and James L. MacKinnon[1]

[1]*Department of Zoology, University of Aberdeen, Tillydrone Avenue, Aberdeen AB24 2TN, UK*
[2]*Biomathematics and Statistics Scotland, Environmental Modelling Unit, Macaulay Land Use Research Institute, Craigiebuckler, Aberdeen AB15 8QH, UK*
[3]*Forest Research, Woodland Ecology Branch, Northern Research Station, Roslin, Midlothian EH25 9SY, UK*

We demonstrate evidence for the presence of travelling waves in a cyclic population of field voles in northern Britain by fitting simple, empirical models to spatially referenced time series data. Population cycles were broadly synchronous at all sites, but use of Mantel correlations suggested a strong spatial pattern along one axis at a projection line 72° from North. We then fitted a generalized additive model to log population density assuming a fixed-form travelling wave in one spatial dimension for which the density at each site was offset in time by a constant amount from a standard density–time curve. We assumed that the magnitude of this offset would be proportional to the spatial separation between any given site and the centroid of the sampling sites, where separation is the distance between sites in a fixed direction. After fitting this model, we estimated that the wave moved at an average speed of 19 km yr^{-1}, heading from West to East at an angle of 78° from North. Nomadic avian predators which could synchronize populations over large areas are scarce and the travelling wave may be caused by density-dependent dispersal by field voles and/or predation by weasels, both of which act at a suitably small spatial scale.

Keywords: spatial patterns; diffusion; dispersal; Mantel correlation; generalized additive models; synchrony

1. INTRODUCTION

Complex spatio-temporal patterns in densities may appear in homogenous environments when diffusion is added to single or multi-species interactions. Systems that are otherwise stable may be destabilized when the stabilizing element in the system diffuses away from perturbations they would otherwise dampen out (Murray 1989; Kareiva 1990). In oscillatory predator–prey systems for instance, random movements of predators and prey result in spatio-temporal oscillations, which may take the form of regular periodic travelling waves (Sherratt *et al*. 1997). However, examples of complex spatio-temporal patterns in natural populations are scarce and predictions on how different degrees of mobility influence spatio-temporal dynamics (de Roos *et al*. 1991) remain untested. The best evidence that spatio-temporal patterns predicted by theory occur in real ecological systems is provided by small vertebrate species with oscillatory dynamics: data from the 'Canadian snowshoe hare enquiry' suggest that snowshoe hare (*Lepus americanus*) dynamics spreads through waves in Canada (Smith 1983; Ranta *et al*. 1997*a*,*b*); anecdotal reports indicate that peaks of wood lemmings (*Myopus schisticolor*) spread westwards in southeastern Norway and western Sweden (Fredga *et al*. 1993); patterns resembling regular travelling waves have been detected in cyclic populations of red grouse (*Lagopus lagopus scoticus*) in Scotland (Moss *et al*. 1999); and an annually moving epicentre of vole plague in Finland and France together with spatial autocorrelation in vole populations are consistent with wave-like pulses in the dynamics of vole populations (Ranta & Kaitala 1997). Gradients in similarity are the only patterns found so far in other vertebrate species with cyclic dynamics, and the spatial scale over which positive cross-correlations in population dynamics are significant ranges from a few to hundreds of kilometres (Sinclair *et al*. 1993; Ranta *et al*. 1995, 1997*a*; Steen *et al*. 1996; Bjørnstad *et al*. 1998). In spatial predator–prey models the scale of prey population synchrony increases with the diffusion rates of a predator (de Roos *et al*. 1991), such that the domain over which homogenous mixing can be assumed can be inferred from the range of distances over which the correlogram is positive (Bjørnstad *et al*. 1998).

Nomadic avian predators operate over large spatial scales in Fennoscandia and they track local rodent populations without delay, hence synchronizing the cyclic fluctuations of voles and lemmings over large areas (Ydenberg 1987; Ims & Steen 1990). In contrast, the dispersal ability of lynx and coyotes relative to their snowshoe hare prey is smaller. Sinclair & Gosline (1997) hypothesized that movements by ground predators emigrating from areas where hare populations have declined account for the travelling wave pattern visible in this species. In this paper, we provide statistical evidence of a regular travelling wave pattern in cyclic populations of field voles in northern Britain, an area where nomadic avian predators are scarcer than in Fennoscandia. We

*Author for correspondence (x.lambin@abdn.ac.uk).

Received 20 April 1998 *Accepted* 6 May 1998

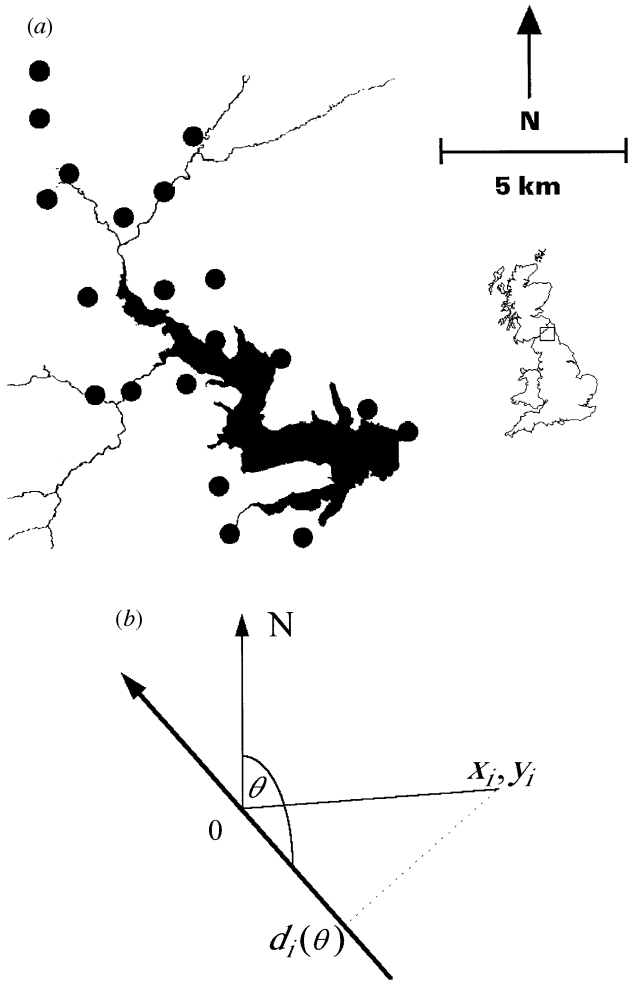

Figure 1. (*a*) Location of sampling sites (circles) in relation to the position of Kielder Water and main valleys. (*b*) Construction of argument of the travelling wave model.

estimate the speed and direction of the travelling wave using spatial autocorrelations and generalized additive models and consider which ecological processes could account for the spatio-temporal pattern.

2. METHODS

Kielder Forest is situated on the border between Scotland and England (55°13′ N, 2°33′ W). It is one of the largest man-made forests in Europe (613 km^2) and consists primarily of Sitka spruce (*Picea sitchensis*) and Norway spruce (*Picea abies*), managed on a 40–60 year rotation. Kielder Forest covers eight valley systems that converge on Kielder Water (a reservoir of 1000 ha; 1 ha = 10^4 m^2) (figure 1). Harvesting of timber (currently 750 ha yr^{-1}) provides well-defined 'islands' of successional habitat that progress from clear-cuts, to grassland, to pre-thicket forest, and finally reaching thicket stage after a period of 12–15 years. Clear-cuts range in size from 5 ha to more than 100 ha. The field vole is common in these ephemeral habitats but absent from forested areas, which lack grass cover. Other small rodent species are scarcer (Petty 1992).

Starting in 1984, one of us (S.J.P.) indexed the abundance of field voles three times a year, in spring (March), summer (May/June) and autumn (September). Between 14 and 18 grass-dominated clear-cuts were selected where mature spruce had been harvested. Before tree growth made sampling sites unsuitable for voles, replacement areas were selected as near to the original as possible (mean distance = 567 m, maximum = 1655 m). Sampling areas were on surface water gleys soils dominated by *Deschampsia caespitosa*, *Agrostis tenuis*, *Juncus effusus*, *Holcus* spp. and bryophytes. At each sampling area, 25 randomly chosen quadrats (25 cm × 25 cm) were scored for the presence or absence of vole signs (fresh green heaps of grass clippings). The position of each quadrat differed between assessments and was determined by walking 15–25 paces from the previous quadrat. A square metal frame was then thrown and the assessment undertaken where it landed. J.L.M. calibrated rapid estimates of vole abundance based on sign indices with actual abundance of field voles estimated by live-trapping at 14 permanent grids (each of area 0.3 ha) in 1996 and 1997 (details in Lambin *et al.* (1999)).

We consider the dynamics of field vole population densities at 21 sites. A full 13-year (1984–1997) series is available for 13 sites and shorter sets for eight sites. Evidence for spatial asynchrony in the vole cycles at each location was assessed by relating cross-correlation between pairs of time-series to distance between pairs of trapping sites using Mantel tests, with statistical significance levels assessed by randomization tests (Manly 1991). Distance between pairs of sites was initially taken as full Euclidean distance, but was later taken as the distance between pairs of sites after projection onto lines of particular angles to North. Mantel correlations were therefore directionally dependent in the same way that semi-variograms may be considered anisotropic in the analysis of spatial data (Cressie 1993). Randomization tests were based on 500 random permutations of time-series to locations.

In the absence of a travelling wave, the temporal means were well modelled by fitting a generalized additive model (GAM) using smoothing splines (Hastie & Tibshirani 1990; Genstat 1993). The fitted equation was of the form

$$\log D(i,t) = m + q(t) + s(t) + e(i,t), \quad (1)$$

where $D(i, t)$ is the observed density at site i and time t, m is the overall mean, $q(t)$ is a seasonal effect depending on whether the observation was made in spring, summer or autumn, $s(t)$ is a smoothing spline describing the temporal fluctuations in population density and $e(i, t)$ are the departures from expectation.

However, a model such as equation (1) can take no account of spatial asynchrony. Our candidate model for spatial asynchrony was based on the travelling wave in one dimension, x, whose general equation is:

$$f(x + ct, t_0 + t) = f(x, t_0), \quad (2)$$

where time is denoted by t and the speed of the wave by c. To fit a model of this type via a GAM, we constructed a modified time argument $t'(i, r, \theta)$ as

$$t'(i,r,\theta) = t + rd_i(\theta), \quad (3)$$

where $d_i(\theta)$ is the distance of site i from the centroid after projection onto a line of angle θ° to North passing through the centroid (figure 1*b*), and where r (yr km^{-1}) $= 1/c$ is the inverse of the speed of the wave. This has the effect of creating a single spatial dimension by projecting the study area onto a line θ° through its centroid. The fitted model was thus

$$\log D(i,t) = m + q(t) + s(t + rd_i(\theta)) + e(i,t). \quad (4)$$

Hence, we assume that a travelling wave in one spatial dimension would result in the density of a site being offset in time from a common trajectory. The magnitude of this offset is

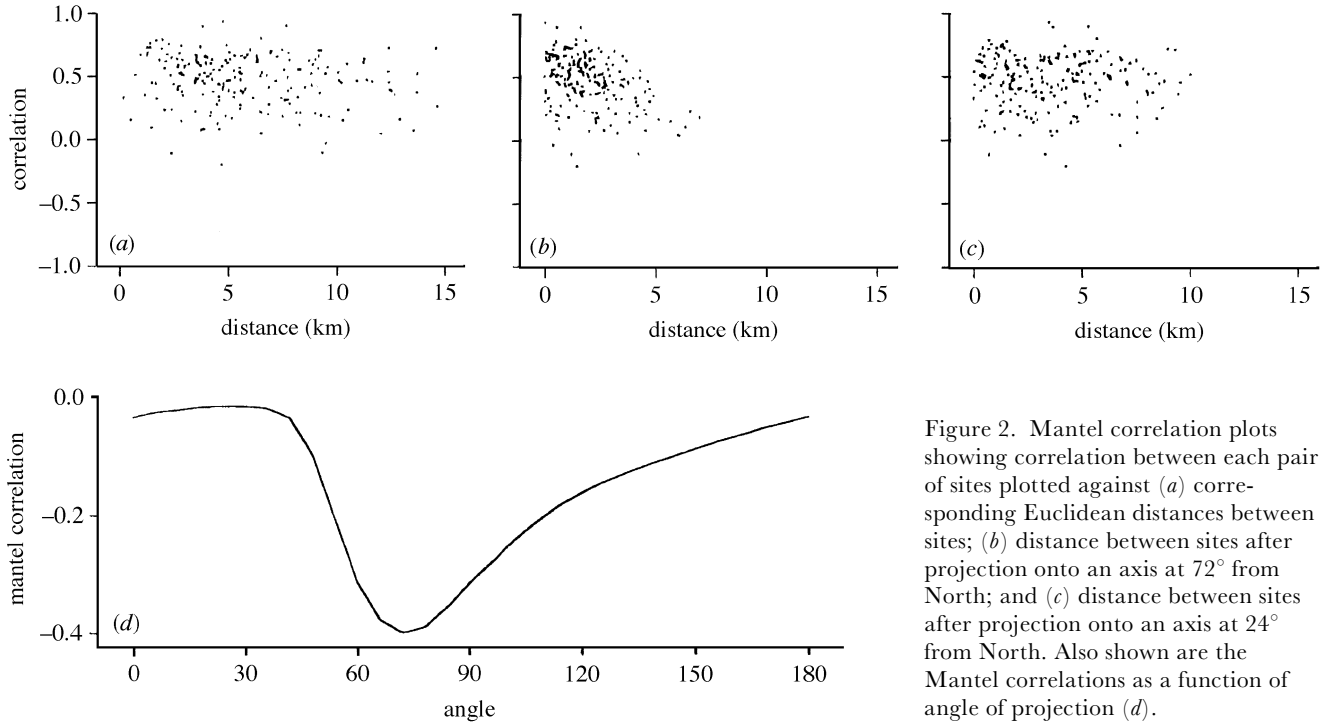

Figure 2. Mantel correlation plots showing correlation between each pair of sites plotted against (*a*) corresponding Euclidean distances between sites; (*b*) distance between sites after projection onto an axis at 72° from North; and (*c*) distance between sites after projection onto an axis at 24° from North. Also shown are the Mantel correlations as a function of angle of projection (*d*).

assumed to depend upon the projected distance between any given site and the centroid multiplied by the reciprocal of the speed of the wave.

The number of degrees of freedom, m, associated with the smoothing spline was selected by repeated fitting of the GAM without the travelling wave (equation (1)) and observing both the reduction in deviance associated with increasing degrees of freedom and the shape of the fitted response curve. The selected value of m was then used for fitting the travelling wave model. All models were fitted by least squares, ignoring correlations in the residuals. With the travelling wave parameters r and θ fixed, the smoothing spline can again be fitted as a GAM. To optimize the fit over the nonlinearly appearing parameters r and θ, we performed iterative quadratic minimization of the residual mean square of fits in the space of the transformed parameters $r\cos(\theta)$, $r\sin(\theta)$. At each iteration, combinations of $r\cos(\theta)$ and $r\sin(\theta)$, selected for evaluating the deviance of the GAM, were the nine design points of a central composite design (Cochran & Cox 1957), centred on the current parameter estimates and with major and minor ellipse axes of length twice the respective standard errors.

The modelling procedure leads to robust parameter estimates but over-optimistic significance levels because the correlations in residuals were ignored. Improved significance levels were obtained by refitting the model to 500 random permutations of time-series to locations. Profile likelihood methods based on the reduction in deviance obtained on adding the two travelling wave parameters are informative, and are displayed as contour plots with confidence ellipses appropriate for standard likelihood ratio tests. However, the nominal significance levels attached to particular confidence ellipses should be taken with caution.

3. RESULTS

Mantel plots suggest some tendency for cross-correlation between time series to decrease with increasing separation of sites (figure 2*a*). The Mantel correlation with respect to Euclidean distance was estimated as -0.16, with $p=0.036$. However, Mantel correlations with respect to projected distance varied markedly with the angle of the line onto which the projection was being made (figure 2*d*). The strongest correlations (-0.40) were negative with projection onto a line at 72° to North (figure 2*b*). Conversely, projection onto lines around 24° to North led to Mantel correlations that were close to zero (figure 2*c*).

The best smoothing spline without the travelling wave was chosen to have 21 degrees of freedom (d.f.), and provides a good fit to the means at each time but without looking too rough (figure 3*a*). The associated residual sum of squares was 336.0 with 705 d.f. Obtaining the maximum likelihood estimates (MLE) for r, θ took five iterations of the central composite algorithm, leading to a residual sum of squares of 323.1 on 703 d.f. and an associated mean square of 0.460. The resulting parameter estimates were $r=0.0536\,\mathrm{yr\,km^{-1}}$ and $\theta=258°$, suggesting there is a travelling wave in relative growth rate heading broadly from West to East at a speed of $19\,\mathrm{km\,yr^{-1}}$. The profile likelihood plot (figure 3*b*) shows confidence ellipses that are long and narrow, reflecting the influence of the layout of sampling sites (figure 1*a*) on parameter estimation. The fit of the travelling wave model to the observed data was better than for any of the 500 randomizations.

The temporal effect on vole abundance does not reach all sites simultaneously. For each of the seasons in years 1990 and 1991, we have plotted the log densities against the location of each site after projection onto a line in the direction of the travelling (figure 4*a–f*). The spatial asynchrony in the data is displayed here as non-zero slopes of the regression of log density on projected distance. The sign of slopes changes from negative (higher vole log density to the west of study area) through zero to positive (higher vole log density to the east of study area) as a

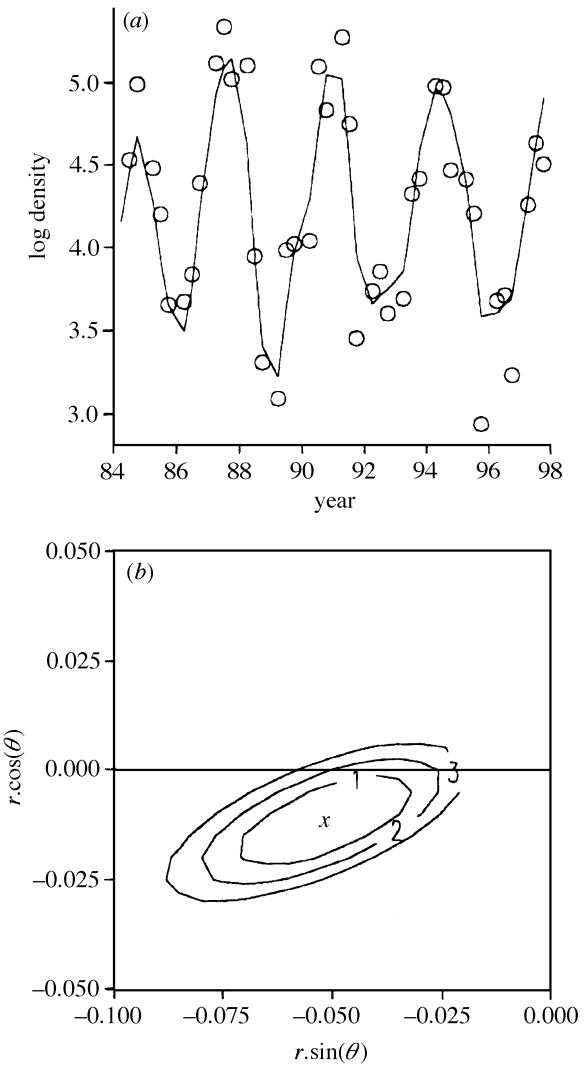

Figure 3. (*a*) Mean values of log density for each observation time (open circles) and fitted smoothing spline (solid line). (*b*) Profile likelihood for the parameters $r\cos(\theta)$ and $r\sin(\theta)$ of the travelling wave model, showing the MLE (x) and contours corresponding to 80%, 95% and 99% confidence intervals.

peak in log density sweeps through Kielder Forest. Figure 4*g* also shows the corresponding estimated values of $m+s(t')$ from the travelling wave model. The slopes of these estimated values track reasonably, but far from perfectly, the changes in slope of the regression of observations on projected location over this limited time period.

A fuller picture of the concordance between data and fitted model can be seen in figure 4*g* where the slopes of the regression of log density on projected location are given for each observation time, along with the slopes of the corresponding regressions for the fitted values. The turning points in these graphs should correspond to periods of peak growth or decline when projected distance has most effect on density, whereas zeros in the graph should correspond to turning points in density when projected distance has least effect. The model predicts greatest asynchrony midway between peaks and troughs in density, which broadly accords with the asynchrony in the data during the cycles that peak in 1989 and 1993. The matching of slopes shows some systematic deviations with greatest asynchrony occurring later than predicted by the model. The peak slopes in the data are also much greater than predicted by the model. This lack of fit can be put into context by recalling that the variation explained by the travelling model had a mean square of 6.4 on 2 d.f. On fitting individual linear regression equations for log density on projected location for the data from each season, the additional variation explained has a mean square of 1.3. Thus, mean square explained by the travelling wave parameters is five times the mean square explained by the unconstrained regressions, indicating the relative importance of the travelling wave parameters.

4. DISCUSSION

There has been much recent interest in relating the degree of synchrony to spatial separation (Sinclair *et al*. 1993; Ranta *et al*. 1995; Steen *et al*. 1996; Bjørnstad *et al*. 1998). Most previous studies have considered the spatial scale over which populations are more similar to each other than they are over an entire region, without explicitly looking for spatio-temporal patterns in abundance or population growth other than gradients. Ranta *et al*. (1997*a*) inferred from the U-shape of the relationship between an index of synchrony in population growth, that hare dynamics spread through waves in Canada. In another study, Ranta & Kaitala (1997) interpreted an annually changing epicentre of vole damage together with positive spatial autocorrelations in vole populations as evidence of travelling waves. The present paper extends the accepted level of analysis in two ways. First, by resolving spatial separation into directional components, we have shown that spatial autocorrelation in time-series can depend on direction of separation as well as Euclidean distance between sites. Second, we have found a method of fitting an empirical model to the data which, unlike previous methodologies, captures the spatio-temporal dynamics and extends readily for non-parallel wavefronts. However, its adaptation to take account of additional demographic variation is less straightforward, as is the adaptation of the estimation to incorporate spatio-temporal variation in the residuals, since this is incompatible with the current implementation of generalized additive models in statistical packages.

There are some systematic departures between the data and the fitted model, which suggest that the observed spatial trends in growth rate of vole density do not arise solely as the result of some common temporal trend sweeping across the landscape at a constant speed (figure 4). Two obvious factors could account for these departures. First, clear-felled patches that are inhabited by field voles have a highly fragmented distribution in Kielder Forest and a large body of water lies in the middle of the study area. If features of the landscape impeded the movement of the wave, any wave would not travel at a constant speed as assumed by our model. Second, the systematic discrepancy between the model assuming a wave of constant speed and the data may indicate that vole density influences the speed of the travelling wave. The model predicts greatest asynchrony in the early stages of population declines and increases,

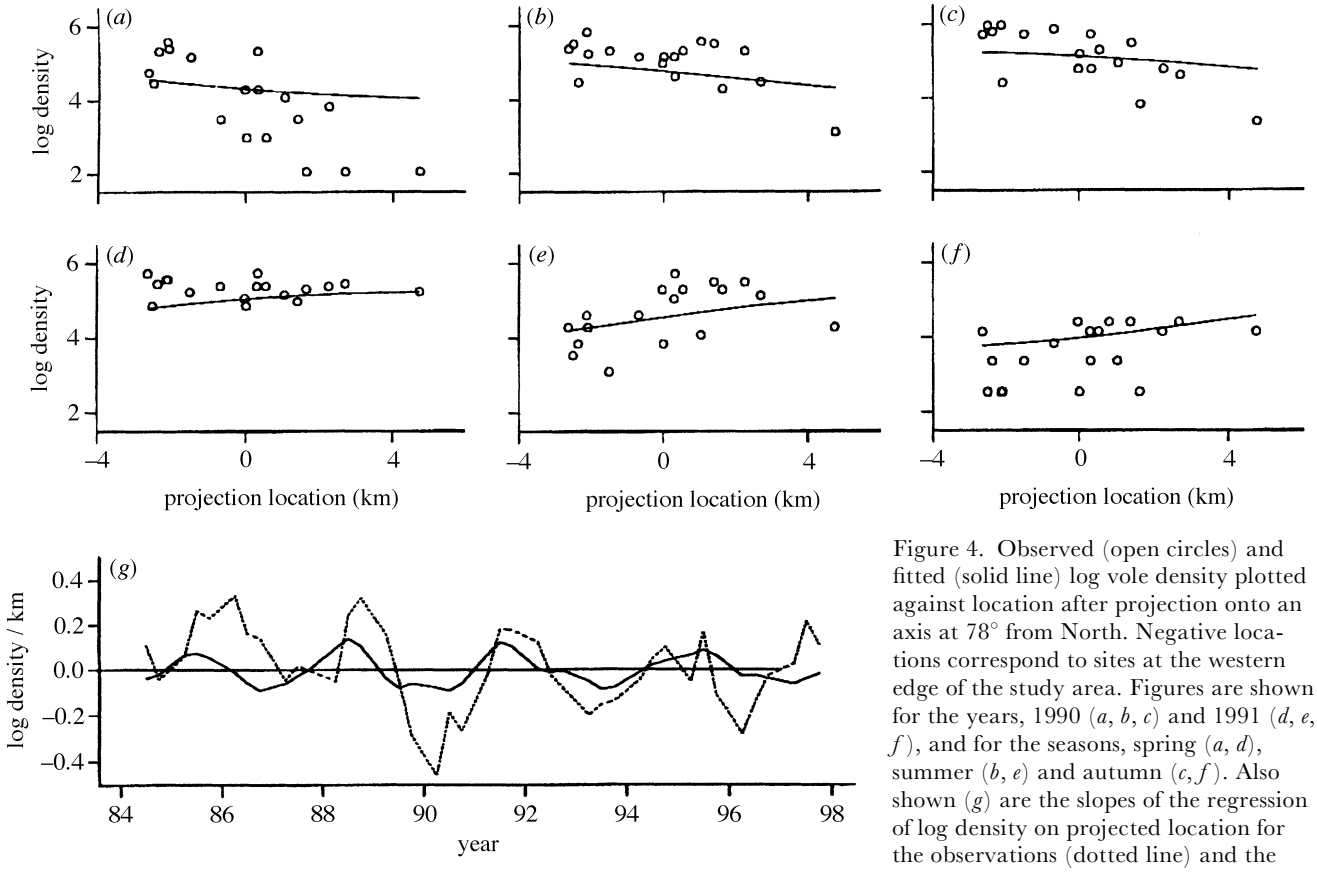

Figure 4. Observed (open circles) and fitted (solid line) log vole density plotted against location after projection onto an axis at 78° from North. Negative locations correspond to sites at the western edge of the study area. Figures are shown for the years, 1990 (*a*, *b*, *c*) and 1991 (*d*, *e*, *f*), and for the seasons, spring (*a*, *d*), summer (*b*, *e*) and autumn (*c*, *f*). Also shown (*g*) are the slopes of the regression of log density on projected location for the observations (dotted line) and the fitted line (solid line) for each sampling time.

but the data suggest that asynchrony was greatest in the later stages of the incline and decline phases of the 3–4-year cycles. Furthermore, the spatial dependency on log density is often greater than predicted by the travelling wave model for any phase of the oscillation. A similar type of phase dependency is visible in the growth pattern of cyclic populations of the snowshoe hare, which appear to spread in waves in Canada (Smith 1983). There was almost complete synchrony between populations in Alberta and Saskatchewan at the end of increase phase and spatial variability was greatest when hare densities were declining or low. Sinclair & Gosline (1997) suggested that any wave was restricted to the decline phase and may be caused by predators such as lynx and coyotes emigrating from areas where hare populations have declined and travelling over large distances. They further speculated that the synchronizing effect of mobile predators could dissipate in the low phase as their numbers drop. This does not appear to be the case in Kielder Forest, as spatial dependency was clearly not restricted to the decrease phase of the cycles of field voles (figure 4). Thus, the ecological process responsible for the travelling wave in field vole population growth is acting throughout the cycle, but its effectiveness appears impeded by high and low vole density.

Analyses using Mantel correlations and generalized additive models imply that the spatio-temporal pattern is effectively unidimensional. The travelling wave's direction of 78° from North could reflect the spatial distribution of grassland patches habitable by field voles if the travelling wave originated within Kielder Forest. Alternatively, if periodic travelling waves swept through a much larger area, its observed direction within Kielder Forest could result from the configuration of field vole habitats at a regional scale. The oscillations of field vole populations in Kershope Forest, which lies 12 km to the south west of Kielder, have been approximately one year out of phase with each other since 1987, consistent with the wave in growth rate of vole populations operating at a regional scale.

Nomadic birds of prey with a capacity for rapid long-distance movements and accurate tracking of local prey are scarcer in Kielder Forest than in Fennoscandia. Thus, in Kielder Forest they failed to synchronize the dynamics of field voles and smaller-scale patterns are revealed. The spatial scale over which positive cross-correlations in population dynamics are significant in Kielder Forest depends greatly on direction. It is five- to tenfold smaller in the direction of the wave (*ca.* 4 km) than estimates from other cyclic vole species in similar habitats in Fennoscandia or northern Japan, implying that the ecological process that generates the dynamic spatial pattern in Kielder Forest has more limited potential to diffuse (Steen *et al.* 1996; Bjørnstad *et al.* 1998). Periodic travelling waves arise in models of predator–prey and plant–herbivore interactions and in single species where dispersal is age dependent (Kareiva 1990; Hasting 1992). Their formation depends upon the relative magnitude of the diffusion parameters of the two components of an activator–inhibitor system. It is therefore not straightforward to estimate the magnitude of diffusion parameters from the speed of the wave, as would be possible under simple diffusion. In

Sherratt *et al*.'s (1997) simulations of the invasion of prey population by predators with oscillatory dynamics, regular periodic spatio-temporal waves occur when prey and predators dispersed at similar rates. We therefore infer that the ecological processes that account for the travelling wave in vole population growth in Kielder Forest should involve components with similar, but limited, dispersal potentials.

Dispersal by field voles may account for contagion between adjacent populations. Dispersal typically takes place over short distances (tens of metres), but its distribution is highly leptokurtic. Contagion through dispersal by several vole generations in each year and the strong age and density dependence of dispersal in voles might be sufficient to create the travelling wave detected in Kielder Forest. Alternatively, weasels (*Mustela nivalis*), which specialize on voles and operate over relatively small spatial scales, could interact with their prey in causing the spatial pattern observed. The timing of greatest spatial asynchrony is consistent with the model predictions on their numerical response to change in vole density, but such predictions are as yet untested. Home range size of weasels varies from 11–216 ha in deciduous forests (Jedrzejewski *et al*. 1995), but corresponding values in Kielder where voles are patchily distributed are presently unknown. Data on patch use in response to vole density are required to determine whether mustelids act as synchronizing agents (Heikkilä *et al*. 1994), or whether weasel–vole interactions could lead to travelling waves in field vole population growth.

We thank Graham Gill, Forest Enterprise, for allowing us to work in Kielder Forest and for providing student accommodation. This project is supported by NERC (GST/02/1218; GT24/95/lspe/2) and the Scottish Office Agriculture, Environment and Fisheries Department.

REFERENCES

Bjørnstad, O. N., Stenseth, N. C. & Saitoh, T. 1998 The scale of population dynamics of voles and mice in Northern Japan. *Ecology*. (In the press.)

Cochran, W. G. & Cox, G. M. 1957 *Experimental designs*, 2nd edn. New York: Wiley.

Cressie, N. A. C. 1993 *Statistics for spatial data*, revised edn. New York: Wiley.

de Roos, A. M., McCauley, E. & Wilson, W. G. 1991 Mobility versus density-limited predator–prey dynamics on different spatial scales. *Proc. R. Soc. Lond.* B **246**, 117–122.

Fredga, K., Fredriksson, R., Bondrup-Nielsen, S. & Ims, R. A. 1993 Sex ratio, chromosomes and isozymes in natural populations of the wood lemming (*Myopus schisticolor*). In *The biology of lemmings* (ed. N. C. Stenseth & R. A. Ims), pp. 465–491. London: Academic Press.

Genstat 5 Committee 1993 *Genstat 5, release 3, reference manual*. Oxford: Clarendon Press.

Hastie, T. J. & Tibshirani, R. J. 1990 *Generalised additive models*. London: Chapman & Hall.

Hastings, A. 1992 Age dependent dispersal is not a simple process: density dependence, stability and chaos. *Theor. Popul. Biol.* **41**, 388–400.

Heikkilä, J., Below, A. & Hanski, I. 1994 Synchronous population dynamics of microtine rodents in Lake Inari in northern Fennoscandia: evidence for regulation by mustelid predators. *Oikos* **70**, 245–252.

Ims, R. A. & Steen, H. 1990 Geographical synchrony in microtine population cycles: a theoretical evaluation of the role of nomadic avian predators. *Oikos* **57**, 381–387.

Jedrzejewski, W., Jedrzejewska, B. & Szymura, L. 1995 Weasel population response, home range, and predation on rodents in a deciduous forest in Poland. *Ecology* **76**, 179–195.

Kareiva, P. 1990 Population dynamics in spatially complex environments: theory and data. *Phil. Trans. R. Soc. Lond.* B **330**, 175–190.

Lambin, X., Petty, S. J. & MacKinnon, J. L. 1999 Cyclic fluctuations in field vole populations in northern England: the roles of predation and habitat fragmentation. *J. Anim. Ecol.* (Submitted.)

Manly, B. F. J. 1991 *Randomization and Monte Carlo methods in biology*. London: Chapman & Hall.

Moss, R., Elston, D. A. & Watson, A. 1999 Spatial asynchrony and demographic travelling waves during red grouse population cycles. *Ecology*. (Submitted.)

Murray, J. D. 1989 *Mathematical biology*. New York: Springer.

Petty, S. J. 1992 Ecology of the tawny owl *Strix aluco* in the spruce forests of Northumberland and Argyll. PhD thesis, The Open University, Milton Keynes.

Ranta, E. & Kaitala, V. 1997 Travelling waves in vole population dynamics. *Nature* **390**, 456.

Ranta, E., Kaitala, V., Linström, J. & Linden, H. 1995 Synchrony in population dynamics. *Proc. R. Soc. Lond.* B **262**, 113–118.

Ranta, E., Linström, J., Kaitala, V., Kokko, H., Linden, H. & Helle, E. 1997*a* Solar activity and hare dynamics: a cross-continental comparison. *Am. Nat.* **149**, 765–775.

Ranta, E., Kaitala, V. & Linström, J. 1997*b* Dynamics of Canadian lynx populations in space and time. *Ecography* **20**, 454–460.

Sherratt, J. A., Eagan, B. T. & Lewis, M. A. 1997 Oscillations and chaos behind predator–prey invasion: mathematical artefact or ecological reality? *Phil. Trans. R. Soc. Lond.* B **352**, 21–38.

Sinclair, A. R. E. & Gosline, J. M. 1997 Solar activity and mammal cycles in the northern hemisphere. *Am. Nat.* **149**, 776–784.

Sinclair, A. R. E., Gosline, J. M., Holdsworth, G., Krebs, C. J., Boutin, S., Smith, J. N. M., Boonstra, R. & Dale, M. 1993 Can solar cycle and climate synchronize the snowshoe hare cycle in Canada? Evidence from tree rings and ice core. *Am. Nat.* **141**, 173–198.

Smith, C. H. 1983 Spatial trends in Canadian snowshoe hare, *Lepus americanus*, population cycles. *Can. Field Nat.* **97**, 151–160.

Steen, H., Ims, R. A. & Sonerud, G. A. 1996 Spatial and temporal patterns of small-rodent population dynamics at a regional scale. *Ecology* **77**, 2365–2372.

Ydenberg, R. 1987 Nomadic predators and geographical synchrony in microtine population cycles. *Oikos* **50**, 270–272.